Cold Spring Harbor Perspectives in Biology
www.cshperspectives.org

# The Complex Ultrastructure of the Endolysosomal System

**Judith Klumperman[1] and Graça Raposo[2,3]**

[1]Department of Cell Biology, University Medical Center Utrecht, Heidelberglaan 100, 3584 CX Utrecht, The Netherlands

[2]Institut Curie, Centre de Recherche, Paris F-75248, France

[3]Structure and Membrane Compartments CNRS UMR144, Paris F-75248, France

*Correspondence:* j.klumperman@umcutrecht.nl; graca.raposo@curie.fr

Live-cell imaging reveals the endolysosomal system as a complex and highly dynamic network of interacting compartments. Distinct types of endosomes are discerned by kinetic, molecular, and morphological criteria. Although none of these criteria, or combinations thereof, can capture the full complexity of the endolysosomal system, they are extremely useful for experimental purposes. Some membrane domain specializations and specific morphological characteristics can only be seen by ultrastructural analysis after preparation for electron microscopy (EM). Immuno-EM allows a further discrimination of seemingly identical compartments by their molecular makeup. In this review we provide an overview of the ultrastructural characteristics and membrane organization of endosomal compartments, along with their organizing machineries.

The endolysosomal network is required for multiple functions and control of cell homeostasis. It is not only reached by endocytic cargo but also by biosynthetic cargoes. It is an intermediate to degradation, but also essential for recycling, signaling, cell polarity, cilia formation, cytokinesis, and migration (Gould and Lippincott-Schwartz 2009; Taguchi 2013). This multitude of functions can only be ensured by an extremely organized ultrastructure. With the increased understanding of how cellular machinery defines endolysosomal subdomains, the nomenclature of the endolysosomal system has also increased in complexity. We start this review, therefore, with a brief introduction of the terminology of the endolysosomal system.

Coated pits and vesicles were described in 1964 (Roth and Porter 1964), and lysosomes were first described by De Duve and Novikoff in the mid-1950s (Novikoff et al. 1956), but the range of organelles in between these beginning and ending stages of endocytosis was only described later (Bhisey and Freed 1971). Electron microscopy (EM) studies by Allen and coworkers on the unicellular ciliate *Paramecium caudatum* revealed the existence of intracellular compartments that could be loaded with the endocytic marker horseradish peroxidase (HRP) (Allen and Fok 1980). These were named

Editors: Sandra L. Schmid, Alexander Sorkin, and Marino Zerial
Additional Perspectives on Endocytosis available at www.cshperspectives.org

 doi: 10.1101/cshperspect.a016857
Cite this article as *Cold Spring Harb Perspect Biol* 2014;6:a016857

"endosomes." Parallel studies in mammalian cells, by Pastan, Willingham, and colleagues, also using HRP, described intracellular vacuoles and tubules involved in the transport of transferrin receptor (TfR) (Gonatas et al. 1977; Goud et al. 1981; Willingham and Pastan 1983). These were called "receptosomes" (Willingham and Pastan 1980). Geuze, Slot, and collaborators introduced immunogold labeling, allowing the quantitative localization of multiple proteins within one EM sample (Geuze et al. 1981). When they localized the recycling asialoglycoprotein receptor together with its ligand destined for lysosomal degradation (Geuze et al. 1983), they identified compartments consisting of a vacuole and multiple associated tubules. These were called compartments involved in the uncoupling of receptors and ligands (CURLs) because the vacuoles accumulated the ligand (for degradation) and the tubules the receptor (for recycling). Today the CURL is known as the "early endosome" (EE), which in addition to receptors and ligands is now known to be reached by virtually all components internalized from the cell surface (see Mayor et al. 2014; Cossart and Helenius 2014).

In the current literature, different nomenclatures are still used to describe the endolysosomal system, which can sometimes cause some confusion. In this review, based on combined ultrastructural and functional knowledge, we propose the following nomenclature: We refer to the vacuolar domains of EEs as sorting endosomes (SEs) and the tubules emerging from SEs as recycling endosomes (REs). Although in some cells (e.g., melanocytes) (see Delevoye et al. 2009), the RE tubules may stay attached while functioning in recycling, more typically they detach from the SE to form a tubular endosomal network (TEN). The term "endosomal recycling compartment" (ERC) is used to designate the peri-centriolar compartment that can be observed only in some cell types. Late endosomes (LEs), also referred to as multivesicular bodies (MVBs), are rounded compartments filled with intraluminal vesicles (ILVs). Lysosomes are the final compartments of the endocytic pathway, with different morphologies depending on the cell type (schematic representation in Fig. 1). Moreover, in the literature, these terms are differently used because most studies involve light microscopy, which does not provide sufficient resolution to detect all of the distinct domains.

## ELECTRON MICROSCOPY OF THE ENDOSOMAL SYSTEM

The complex membrane structure of endosomes can only be fully comprehended using EM techniques. Here we give a brief description, together with their pro's and con's, of the main types of EM technologies that are applied to explore the endolysosomal system. For a more elaborate overview of these techniques, we refer to the review by van Weering et al. (2010).

### Classical Electron Microscopy

The subcellular organization of membrane-bound organelles has been appreciated through decades by "conventional" or "classical" EM, which involves chemical fixation of cells and tissues, dehydration, embedding in resins, and ultrathin sectioning. The protocols for resin embedding have remained basically unchanged for more than 50 years! However, at present, in addition to chemical fixation, an alternative to optimally preserve the ultrastructure of organelles is high-pressure freezing (HPF), followed by freeze substitution (Studer et al. 2001; Hawes et al. 2007). HPF, however, requires sophisticated equipment, is not easily combined with cytochemical or immunocytochemical methods, and requires expertise such as perfect vitrification of water present in the samples, which is not easily or routinely achieved.

### Cytochemistry and Immunoelectron Microscopy

Cytochemistry, allowing detection of endogenous (acid phosphatase, tyrosinase) enzymatic activities, has been used to define the organelles where these enzymes are present within the endolysosomal system (Shio et al. 1974; Novikoff and Novikoff 1977). In addition, uptake of exogenous enzymes, like horseradish peroxidase

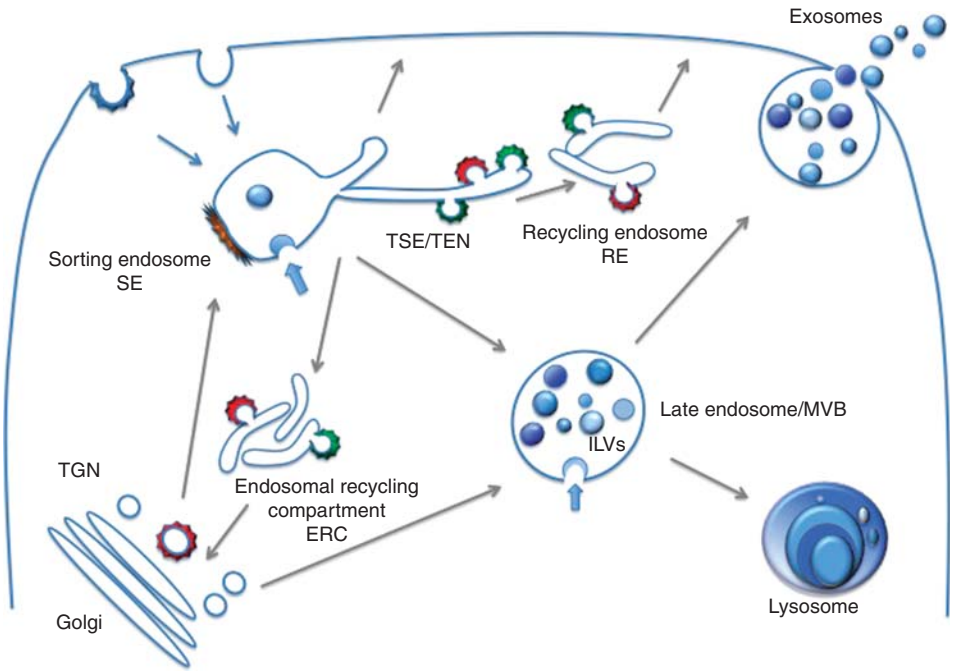


**Figure 1.** Schematic and simplified representation of the endolysosomal system showing the different organelles described in this article. Sorting endosomes (SE) are vacuolar compartments often bearing bilayered, flat clathrin coats (brown). Tubules emanate from SE that form the recycling endosomes (RE). The RE may localize to the *peri*-Golgi area forming the endocytic recycling compartment (ERC) or distribute to the cell periphery. The RE network is complex with multiple sorting sites, thereby the tubular sorting endosome (TSE) or tubular endosomal network (TEN) is also represented. AP1 (red) and AP3 (green) coated buds on RE (ERC/TSE/TEN) are shown. Late endosomes correspond to multivesicular bodies (MVBs) filled with intraluminal vesicles (ILVs). MVBs are fated for fusion with lysosomes. In some cells, a population of MVBs fuse with the plasma membrane, a process during which the ILVs are secreted as exosomes. Gray arrows indicate directions of transport/maturation of compartments. Blue arrows indicate invagination at the endosomal membrane of SE and MVBs required for ILV formation.

(HRP) alone or coupled to a ligand such as transferrin (Tf) or a lectin, has been instrumental in EM studies on endocytosis (Allen and Fok 1980; Willingham and Pastan 1983; Tooze and Hollinshead 1991; Ranftler et al. 2013). HRP is also of use for whole-mount EM, a method by which cross-linking of internalized Tf-HRP preserves endosomal integrity after removal of cytosolic proteins by permeabilization (Stoorvogel et al. 1996). However, although sensitive and easily visualized, the electron-dense product that accumulates after adding an enzyme's substrate often masks membranes and does not allow quantitative analysis, which limits its use.

Immunoelectron microscopy (IEM) methods allow simultaneous visualization of up to three components by using antibodies marked with specifically sized gold particles (Slot and Geuze 1981). The distribution of the gold particles yields invaluable information on the relative enrichment of different components on endosomal subdomains (Geuze et al. 1983; Slot et al. 1988; Slot and Geuze 2007). Toxins and lectins that bind to lipids and glycolipids can also be used for IEM when conjugated to proteins—for example, biotin—that can be recognized by antibodies (Möbius et al. 2002). An important feature of endolysosomal organelles is their pH (see also Maxfield 2014). A

method for pH analysis by IEM is the use of the weak base 3-(2,4-dinitroanilino)-3′-amino-*N*-methyldipropylamine (DAMP) that accumulates in acidic compartments and can be localized by IEM using antibodies against dinitrophenol (DNP) (Anderson et al. 1984). A general drawback of IEM techniques is their relatively low sensitivity. As calculated by Griffiths and colleagues (Griffiths 1993), one gold particle represents approximately 100 molecules!

The use of hydrophobic resins (Lowicryl, LR White) for IEM is only suitable to visualize very abundant components because of epitope masking by the resins. This approach is extensively used for yeast (Romao et al. 2008) and *Caenorhabditis elegans* (Muller-Reichert et al. 2003) and is compatible with preservation by HPF, but it should be noted that the protocols are lengthy and the resins can cause allergies. When IEM is combined with the Tokuyasu ultrathin cryosectioning technique, most antigens retain their antigenicity (Slot and Geuze 2007). Moreover, because antibodies can to some extent penetrate into the section, labeling efficiency is improved over resin sections. Together with an excellent membrane visibility, this makes cryosectioning the IEM method of choice to study the endolysosomal system (Raposo et al. 1997; Slot and Geuze 2007).

### Electron Tomography

In addition to conventional EM and IEM, a better view of the complex ultrastructure of the endosomal network is given by adding the third dimension by electron tomography (ET) (for review, see Koster and Klumperman 2003). Combined with HPF and freeze substitution in resins, it is the method of choice to establish contacts and continuities between endosomal (sub)compartments and other organelles. Methods combining HPF, IEM, and ET are available but have not yet been fully exploited to study the endolysosomal system (Zeuschner et al. 2006; Konig et al. 2007). Combining ET with protocols that impose permeabilization of cells should be interpreted with some care regarding the impact on membrane integrity and structural preservation.

### Correlative Light Electron Microscopy

Most light microscopy (LM) studies on the endolysosomal system use fluorescent probes. These can give dynamic information in living cells or provide a wide field of view that EM is lacking. However, they only visualize fluorescently labeled components and do not provide information on membrane composition or cellular context. Optimally one would like to investigate a sample from fluorescence to EM, or even ET, to identify the nature and morphology of the dynamic structures observed by live-cell imaging or peculiar fluorescent patterns seen in fixed cells. This can be accomplished by correlative light electron microscopy (CLEM) (for review, see van Rijnsoever et al. 2008; Kukulski et al. 2012a,b; Mironov and Beznoussenko 2012; Muller-Reichert and Verkade 2012; Polishchuk et al. 2012). Extrapolation of live-cell data to the EM, however, is not trivial, because three-dimensional (3D) images obtained by LM are very different from ~70-nm sections and retracing single endosomes is experimentally challenging. Moreover, the antibodies that are used for IF do not always work for IEM because of differences in sample preparation or limited numbers of antigens. Ongoing developments in hardware and software aim to increase the throughput of CLEM, and novel labeling probes are designed to extend CLEM to 3D-ET. One exciting example is the genetically encoded probe "miniSOG," a small (106-residue) fluorescent flavoprotein that when illuminated by blue light generates singlet oxygen, which can polymerize diaminobenzidine into an electron-dense precipitate that is easily observed by EM (Shu et al. 2011). Such optimized CLEM methods will be especially powerful for studies on the endolysosomal system with its multitude of dynamic, pleiomorphic membranes.

## EARLY ENDOSOMES

Endocytosis starts with the formation of small, ~60- to 120-nm, clathrin-coated and non-

clathrin-coated endocytic vesicles that bud from the plasma membrane (Mayor and Pagano 2007). The internalized cargo is then almost instantly transported to a network of hundreds of dynamically interacting endosomes located at the cell's periphery, the early endosomes (EEs). EEs receive internalized ligands, for example, Tf and its receptor internalized by clathrin-coated pits, but also bovine serum albumin (BSA) coupled to gold internalized by pinocytosis, as soon as within 1–5 min of internalization (for review, see Trowbridge 1991; Sachse et al. 2002a). The commonly accepted model is that endocytic vesicles fuse with preexisting EEs, which results in the transfer of cargo and addition of membrane. Because EEs also receive biosynthetic vesicles from the *trans*-Golgi network (TGN), their size must be tightly regulated. This is maintained by balancing the incoming traffic with recycling pathways that retrieve membrane and proteins from the EEs (see below).

EEs undergo homotypic fusion (Gorvel et al. 1991; Rybin et al. 1996) and maturation (Stoorvogel et al. 1991), or conversion, into late endosomes (LEs) (Rink et al. 2005). The key protein in the formation, functioning, and fusion of EEs is the small GTPase Rab5 (Zerial and McBride 2001; Wandinger-Ness and Zerial 2014). Depletion of Rab5 from mouse liver led to a marked decrease in the number of EEs and consequently also of LEs, illustrating the intricate and dynamic relationship between these subtypes of endosomal compartments (Zeigerer et al. 2012).

## EE Ultrastructure

EEs are highly dynamic and pleiomorphic organelles, but the typical design is a central vacuole of ~100–500 nm diameter, from which multiple tubules extend (Fig. 2). The vacuole is often referred to as a sorting endosome (SE) because this is the site where endocytosed cargo is sorted for degradation or recycling. The extending tubules are referred to as recycling endosomes (REs). A salient characteristic of EEs is a cytoplasmic clathrin coat that covers parts of the SE membrane (Fig. 2) (Raiborg et al. 2001; Raposo et al. 2001; Sachse et al. 2002b). The content of the SE vacuole is predominantly electron lucent, with occasionally a few intraluminal vesicles (ILVs), which range in size from 40 to 100 nm. ET applied to various mammalian cell types preserved by HPF revealed that these ILVs represent free vesicles, with no connections to the vacuolar membrane (Murk et al. 2003a; Hurbain et al. 2008). The presence of ILVs is restricted to the vacuole, and they are absent from the emerging tubules (Fig. 2).

The typical morphological features of EEs can be distinguished in all TEM preparation methods used to date, but it should be noted that EEs are relatively susceptible to fixation artifacts (Murk et al. 2003b). In HPF-fixed cells SEs appear as football-shaped organelles with an incidental short tubule. In aldehyde-fixed cells, SEs are smaller and more irregularly shaped, while the associated tubules are slightly longer. This aldehyde effect can be reduced by using specific buffers yielding low osmolarities (Murk et al. 2003b).

## The Bilayered Flat Clathrin Coat

A clathrin coat on the SE vacuole has been seen in many different cell types albeit with different frequencies. In some cell types (e.g., melanocytes, which are highly specialized pigment-producing cells), the coat is especially abundant (Fig. 2) (Raposo et al. 2001; van Niel et al. 2011). In ultrathin EM sections of HeLa cells, 30% of the EEs display a coat (Sachse et al. 2002b). The coat, however, is not restricted to EEs, because 6.5% of the LEs also displayed a coat (Sachse et al. 2002b). 3D-ET (Murk et al. 2003a) revealed that the coat consists of oval-shaped patches with a diameter from 80 to 500 nm and that one SE can contain multiple coats. The coat does not extend toward the cytoplasm but is either flat or has a shallow indentation toward the endosomal lumen (Fig. 2). Cross sections through the coat, as observed in transmission EM, show that it is composed of two layers—a bilayered coat—with a dark layer aligning the endosomal membrane and a fuzzy layer facing the cytoplasm (Raposo et al. 2001; Sachse et al. 2002b). This bilayered appearance is characteristic for the endosomal coat and not seen at any

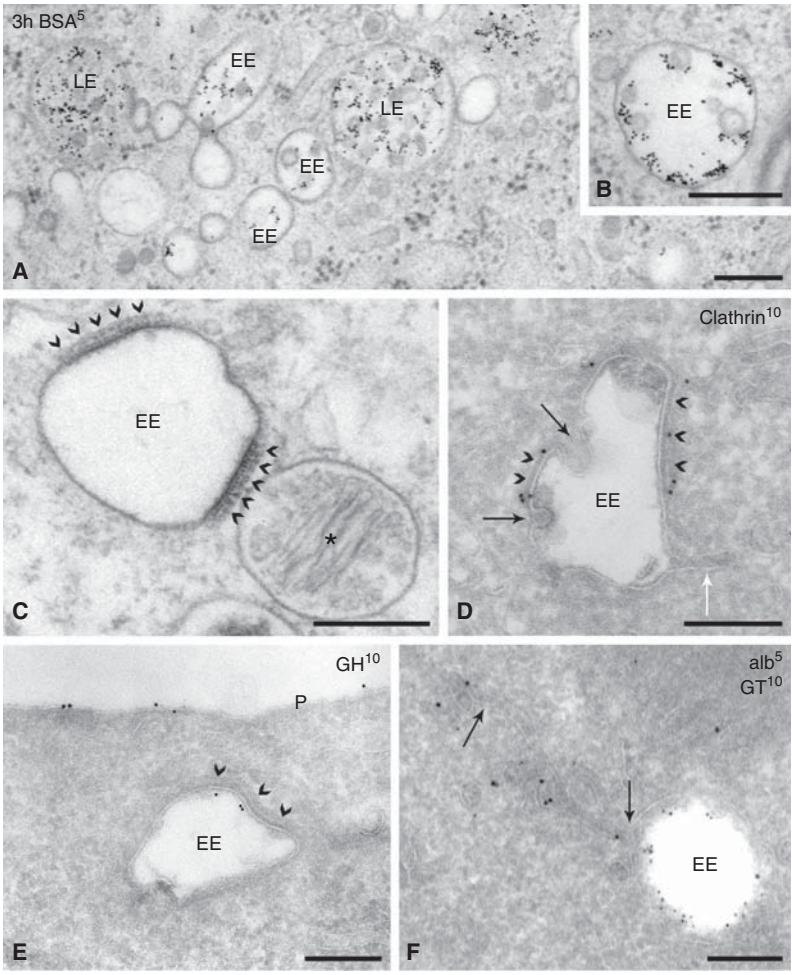


**Figure 2.** Picture gallery of early endosomes. (*A*) HepG2 cells pre-incubated for 3 h with BSA conjugated to 5-nm gold ($BSA^5$). Both early endosomes (EEs) and late endosomes (LEs) are seen. EEs have an electron lucent content with some intraluminal vesicles (ILVs). LEs contain multiple ILVs. (*B*, *inset*) An enlargement of an EE clearly showing that internalized $BSA^5$ is not present in ILVs, which contain cytosolic content. (*C*) Melanocytic cell line analyzed by conventional electron microscopy. Bi-layered coats (arrowheads) are abundant on EEs. Note their typical appearance with an electron-dense layer lining the endosomal membrane and the fuzzier, clathrin-containing layer facing the cytoplasm. (*, on the *right*) A pre-melanosome with intraluminal fibrils. (*D*) EE from a CHO cell immunogold-labeled for clathrin (10-nm gold). Labeling is present on the coated areas of the limiting membrane (arrowheads). Budding of ILVs occurs at the edges of the coat (dark arrows). (White arrow) Points to a recycling tubule extending from the uncoated region of the endosomal membrane. (Adapted from Sachse et al. 2002b, with permission from the author.) (*E*) Internalized growth hormone (10-nm gold) selectively localizes to the part of the endosomal membrane that is covered by the clathrin-coat (arrowheads). This EE does not yet contain ILVs. (From Sachse et al. 2002a; adapted, with permission, from the author.) (*F*) EE in brown adipose tissue immunogold-labeled for albumin (5-nm gold) and Glucose Transporter 4 (10-nm gold). Note the separation of albumin label, in the EE vacuole, and GT label in the emerging recycling tubule (arrows). (Based on Slot et al. 1991; courtesy of Hans Geuze.) Techniques used: (*A*,*B*) HPF and EPON embedding; (*C*) chemical fixation and EPON embedding; (*D*–*F*) chemical fixation and ultrathin cryosectioning. P, Plasma membrane. Scale bar, 200 nm.

other clathrin-coated membrane in the cell. How clathrin triskelions are organized in these coats remains unknown.

The presence of clathrin in the endosomal coats was first described by Reggio, Louvard, and collaborators, referring to the coats as "plaques," when the researchers described the localization of clathrin in cells with one of the first developed monoclonal antibodies (Louvard et al. 1983). By IEM the clathrin was attributed to the outer layer of the coat (Raposo et al. 2001; Sachse et al. 2002b). The striking electron density of the inner layer is indicative of high protein concentrations. Apart from cargo proteins (see below), the endosomal SNARE protein syntaxin 7 is the only protein found to be concentrated in this inner layer (Prekeris et al. 1998; Sachse et al. 2002b), but the functional implication of its presence is not known.

The function of the coat remained enigmatic until several studies showed that it contains high amounts of Hrs and STAM (Raiborg et al. 2002; Sachse et al. 2002b; van Niel et al. 2011; G Raposo et al., unpubl.) and that overexpression of Hrs induces the recruitment of clathrin (Raiborg et al. 2001). Hrs and STAM are components of the endosomal sorting complex required for transport (ESCRT), in particular, of ESCRT-0. Other ESCRT components have not as yet been detected in the coat, possibly because of epitope masking in this area. The ESCRT machinery mediates ubiquitin-dependent incorporation of cargo from the outer membrane of the SE into ILVs (see Henne et al. 2013). By IEM it was shown that cargo molecules destined for lysosomal degradation, such as EGFR, growth hormone receptor, and the melanosomal proteins MART-1 and OA1, are concentrated in the coat, but recycling proteins like TfR are not (De Maziere et al. 2002; Sachse et al. 2002b; Giordano et al. 2011). Ubiquitination of TfR redirects this protein from the recycling to the degradative pathway and its localization from uncoated to coated areas of the SE, dependent on the Hrs ubiquitin interacting domain (Raiborg et al. 2002; Urbe et al. 2003). Thus, ubiquitinated cargo is concentrated in the SE clathrin coats before sorting into ILVs. Sorting into ILVs prevents cargo from following the default recycling pathway to the plasma membrane and targets it for lysosomal degradation (Sachse et al. 2002b; Huotari and Helenius 2011).

## ILV Formation

Both two-dimensional (2D) and 3D-ET studies have shown that ILV formation occurs at the edges of the clathrin-coated regions, suggesting that coat disassembly must occur before ILV formation can proceed (Sachse et al. 2002b; Murk et al. 2003a). By IEM, Hrs and clathrin were not found in ILVs, and biochemical studies showed that after completion of their sorting function, ESCRT complexes are released from the membrane by VPS4 (Babst et al. 1998). Overexpression of a VPS4 mutant resulted in extended coats on enlarged SE vacuoles with reduced numbers of ILVs (Sachse et al. 2004), showing a direct relationship between the coat and ESCRT machinery. Some ESCRT components (Tsg101) and accessory proteins (Alix), however, have been found by proteomics analysis in exosomes, which are ILVs released into the extracellular space after endosome fusion with the plasma membrane (Fig. 1) (for review, see Raposo and Stoorvogel 2013). Some components of the ESCRT sorting machinery may therefore be incorporated into ILVs upon dissociation. These data cannot be extrapolated to yeast, in which the ESCRT machinery is essential for ILV biogenesis (Odorizzi et al. 1998), but no evidence is obtained for an endosomal clathrin coat. The coat may have evolved in higher organisms to accommodate the higher complexity of sorting mechanisms.

Unlike in yeast, in mammalian cells, there is evidence for several ESCRT-independent machineries that can drive ILV formation. Cells in which four subunits of the ESCRT complexes were concomitantly inactivated still display LEs filled with ILVs positive for CD63 (Stuffers et al. 2009), a tetraspanin that is highly enriched on ILVs (Pols and Klumperman 2009). A role for CD63 in ESCRT-independent sorting was proposed by studies in melanocytes. Sequestration of the melanosomal protein PMEL into ILVs does not require ubiquitination and is insensitive to inhibition of Hrs or Tsg101 (Theos et al.

2006) but depends on the presence of CD63 (van Niel et al. 2011). Depletion of CD63 is accompanied by an increase of the Hrs/clathrin coats, in agreement with an increase in ESCRT-dependent degradation of PMEL (van Niel et al. 2011).

These studies stress a tight balance between ESCRT-dependent and -independent mechanisms within the endosomal membrane. Such balance is probably critical to determine the fate of cargoes that are destined for either specialized organelles (i.e., the melanosome) or degradation (i.e., the lysosome). Other factors proposed to be involved in ESCRT-independent ILV biogenesis are the lipids LBPA (2,2′-dioleoyl lysobiphosphatidic acid) and ceramide, both of which can drive ILV formation in vitro (Matsuo et al. 2004; Trajkovic et al. 2008). For a detailed description of the machineries involved in ILV formation, we refer you to Bissig and Gruenberg (2013).

## LATE ENDOSOMES

Late endosomes (LEs) mature from the SE vacuole (Stoorvogel et al. 1991). By live-cell microscopy following individual compartments, it was shown that an individual endosome can exchange Rab5 for Rab7 to mature into an LE (Rink et al. 2005). This model was recently supported by following LDL as a cargo (Foret et al. 2012). However, a viral cargo (Semliki Forest virus) was reported to be sorted in a different manner from Rab5-positive EEs to Rab7-positive LEs (Vonderheit and Helenius 2005). In any case, once formed, LEs are competent to fuse with lysosomes (Mullock et al. 1998).

### LE Ultrastructure

By EM, LEs appear as globular vacuoles of 250–1000 nm in diameter (Fig. 3). They display membrane tubules or buds representing various recycling pathways, which lead predominantly to the *trans*-Golgi network (TGN) (Rojas et al. 2008). Depending on the cell type, LEs are reached by endocytic tracers between 5 and 30 min (for review, see Sachse et al. 2002a). Both by chemical and HPF fixation, the LE vacuole is characteristically round to oval shaped (Murk et al. 2003b), with some patches of clathrin coat, indicating that protein sorting and ILV formation continue at this stage (Sachse et al. 2002b).

Many EM studies use the increasing number of ILVs as an ultrastructural tool to position a compartment within the endolysosomal pathway (Futter et al. 1996; Kleijmeer et al. 2001b; Mari et al. 2008). For some cells—for example, HepG2, dendritic cells (DCs), and HeLa cells—the number of ILVs was directly correlated to the occurrence of marker proteins like Rab5 or Rab7, mannose-6 phosphate receptors, EGFR, LBPA, and LAMP (Futter et al. 1996; Kobayashi et al. 1998; Kleijmeer et al. 2001b). This approach pinpointed the switch from EEs to LEs at five to eight ILVs (Kleijmeer et al. 2001b; Möbius et al. 2003; Murk et al. 2003b; Mari et al. 2008). Interestingly, markers that are considered specific for EEs show different distributions. For example, EEA1 localization is restricted to very-early-stage EEs, whereas Rab4 is more widely spread (Mari et al. 2008). For a substantial list of the changes accompanying the "aging endosome," see the reviews by Saftig and Klumperman (2009) and Huotari and Helenius (2011).

The increased number of ILVs gives LEs a characteristic appearance, and hence they are commonly called multivesicular bodies (MVBs) or multivesicular endosomes (MVEs), as described initially by Sotelo and Porter (1959) (for recent review on MVBs, see Hanson and Cashikar 2012). The term "MVB," however, is still a topic of some debate. In most studies, it is used as a synonym for LEs. Others, however, use it to indicate an intermediate that forms from the SE in order to fuse with an LE. By this definition, the MVB is positioned before LEs (for review, see Gruenberg and Stenmark 2004). Some investigators also make a distinction between early and late MVBs, depending on the number of ILVs (e.g., White et al. 2006). The unifying factor in these definitions is that an increasing number of ILVs reflects the temporal progression along the endolysosomal pathway. In this review, we use the term "MVB" as a synonym for "LEs."

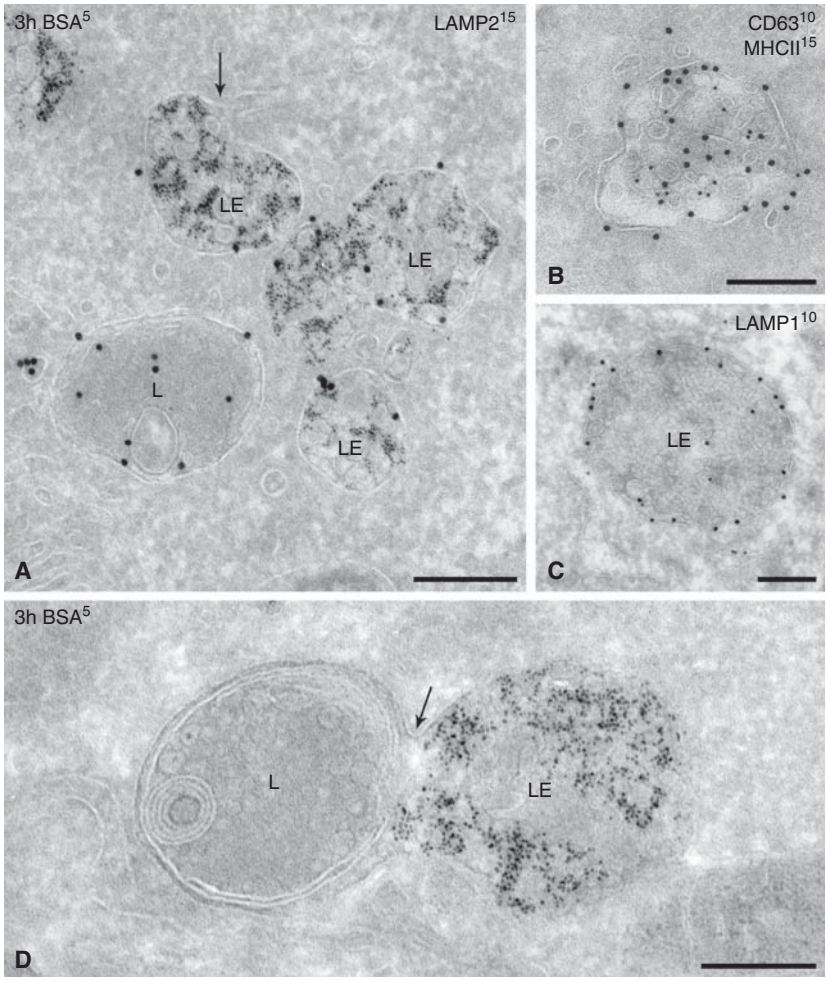


**Figure 3.** Picture gallery of late endosomes. (*A*) HepG2 cells pre-incubated for 3 h with $BSA^5$ and immunogold-labeled for LAMP2 (15-nm gold particles). LE vacuoles contain multiple ILVs but can differ in size and shape. Note the recycling tubule emerging from the LE (arrow). The lysosome (L) has not been reached by $BSA^5$. (*B*) MVB/MHC class II compartment of a dendritic cell immunogold-labeled for MHC class II (15-nm gold) and CD63 (10-nm gold). Note that the ILVs are heterogeneous in size. CD63 is rather associated with smaller vesicles, whereas MHC class II is present on the larger vesicles and also with the limiting membrane. (*C*) Typical example of an LE/MVB. Immunogold labeling for LAMP1 (10-nm gold) is mainly restricted to the limiting membrane. Note the different morphological features of the ILVs present in these distinct MVBs (*A–C*). (*D*) HepG2 cells pre-incubated for 3 h with $BSA^5$. Fusion profile (arrow) of an LE positive for $BSA^5$ with a lysosome devoid of $BSA^5$. Techniques used: (*A–C*) Chemical fixation and ultrathin cryosectioning; (*D*) HPF, rehydration, ultrathin cryosectioning. Scale bar, 200 nm.

## Distinct Populations of LEs/MVBs

An interesting question is whether the multiple machineries for ILV formation result in multiple types of MVBs. The answer is probably yes. For example, lyso(bis)phosphatidic acid (LBPA), which in vitro induces the formation of ILVs in giant unilamellar membranes (Matsuo et al. 2004) and is present in lysosomes (Möbius et al. 2003) and a subpopulation of MVBs. Importantly, the LBPA-MVBs are distinct from morphologically identical EGFR-

containing MVBs, which are specifically induced by EGF uptake (White et al. 2006). Moreover, the phosphatidylinositol (PI)3-kinase Vps34 is required for ILV generation only within the EGFR-MVBs (Bright et al. 2001; Futter et al. 2001). Both EGFR and LBPA endosomes contain CD63, which—as mentioned above—is also involved in ILV biogenesis (van Niel et al. 2011). In addition, the localization of cholesterol, with the toxin perfringolysin, has enabled identification of two populations of MVBs, one cholesterol rich and another with only low amounts of cholesterol (Möbius et al. 2002). Interestingly, the cholesterol-enriched MVBs appeared to fuse more frequently with the plasma membrane (Möbius et al. 2002).

Further support for the existence of multiple types of MVBs comes from dendritic cells (DCs) (described in more detail in ten Broeke et al. 2013). Here, the mode of sorting MHCII into ILVs varies with activation status. In immature DCs, MHCII sorting requires ubiquitination and results in lysosomal degradation (van Niel et al. 2006). In activated DCs, MHCII sorting is ubiquitin-independent and results in sorting to ILVs of smaller-sized, CD9-positive MVBs with the ability to fuse with the plasma membrane and secrete their ILVs as exosomes (Buschow et al. 2009). These data indicate the presence of two populations of MVBs: one for lysosomal targeting and the other for exosome secretion.

The existence of morphologically identical but molecularly distinct endosomes has important consequences for the interpretation of morphological data. For example, by immunofluorescence microscopy, only that subpopulation of endosomes that contains a specific marker will light up. By EM, all subtypes (characterized by size, presence or not of cytosolic coat, particular morphology, and size of the ILVs) can be seen. Molecular differences between these organelles, however, can only be appreciated by IEM. There is also evidence that the content of one MVB is heterogeneous, with ILVs of different sizes and cargo (Fig. 3) that likely reflect different machineries of sorting to ILVs as discussed above.

## Endoplasmic Reticulum-LE/MVB Contacts

Both EEs and LEs can form contact points with ER cisternae, which provide sites for lipid exchange and protein–protein interaction. One endosome can have multiple contact sites, consisting of a parallel arrangement of membranes that can extend to several hundreds of nanometers (Eden et al. 2010). EGF endocytosis tends to induce an increase in the length of ER–endosome contacts, providing putative interaction sites for endocytosed EGFR and the protein tyrosine phosphatase PTP1B (Eden et al. 2010). When endosomes mature, they appear to become more tightly associated with the ER (Friedman et al. 2013), which is important for dynein-mediated transport of endosomes over microtubules regulated by Rab7-interacting lysosomal protein (RILP) (Jordens et al. 2001). RILP recruits dynein motor complexes to Rab7-containing LEs and lysosomes as well as the oxysterol-binding protein-related protein 1 L (ORP1L) (Johansson et al. 2007). Under low cholesterol conditions, ORP1L induces formation of ER–LE contacts that allow interaction between RILP and the ER protein VAP (VAMP [vesicle-associated membrane protein]–associated ER protein) (Rocha et al. 2009). This interaction prevents complex formation between RILP and dynein, resulting in movement of LEs to the microtubule plus-ends. Under high cholesterol conditions, a conformational change in ORP1L prohibits VAP–RILP interactions, which allows RILP to interact with the dynein machinery resulting in the delivery of LEs to the peri-nuclear area. These data explain how the ER and cholesterol control the association of LEs with motor proteins and their positioning in cells.

These ER–endosome connections are reminiscent of the early GERL concept (Golgi–ER–lysosome) proposed by Novikoff (for review, see Novikoff and Novikoff 1977). Although not a site for lysosome biogenesis, as was originally proposed for GERL, the intricate and important relationship between these two compartments was recognized in these early studies. LEs that move to the peri-nuclear area can undergo homotypic or heterotypic fusion with lysosomes

(Luzio et al. 2010). The latter fusion events can result in transient LE–lysosome hybrid organelles (Fig. 3) (Futter et al. 1996; Luzio et al. 2010; Huotari and Helenius 2011).

## LYSOSOMES

In addition to endocytosis, lysosomes receive—directly or indirectly via endosomes—membrane and functional lysosomal proteins from the biosynthetic pathway. Two main pathways for delivery of lysosomal proteins are the established mannose-6-phosphate receptor (MPR)–mediated, clathrin-dependent pathway for lysosomal enzymes (for review, see Saftig and Klumperman 2009) and the recently discovered Vps41/VAMP7-dependent pathway specific for lysosomal membrane proteins (Pols et al. 2013). Finally, lysosomes are also supplied with cargo and membranes from the autophagy pathway—the process whereby intracellular components are sequestered by double-membrane vesicles that fuse with the endolysosomal pathway to form autolysosomes. Autolysosomes are generally larger and more irregularly shaped than lysosomes, with a highly variable content in which sometimes remnants of cytoplasmic components, for example, ribosomes, mitochondria, are seen (Fig. 4). See Eskelinen et al. (2011) for a recent overview on ultrastructural studies in the autophagy field and Tooze et al. (2014) for an overview of the functional relationship between the autophagic and endocytic pathways.

### Lysosome Ultrastructure

Lysosomes generally appear as spherical organelles, with diameters between 200 nm and >1 μm (Fig. 4) (Bainton 1981). Their size and shape are similar in chemical and HPF-fixed cells (Murk et al. 2003b). The presence of a clathrin coat is sporadic, although AP2 coats have been reported to assemble onto lysosomes (Traub et al. 1996). The content of a lysosome varies with the type and quantity of the cargo that is supplied and its degree of degradation, but is typically electron-dense, reflecting high protein concentrations. In live cells, tubules extending from lysosomes can be visualized. These extend in a microtubule-dependent manner to endosomes, exchanging content by kiss-and-run before full fusion, likely to recycle components not fated for degradation (Bright et al. 2005).

The main function of lysosomes is the degradation of their cargo into products that can transfer to the cytoplasm for metabolic reuse. Glycoproteins and oligosaccharides, but also the membranes provided by the ILVs, are degraded in lysosomes (Kolter and Sandhoff 2010). In many cells, such as HeLa, ILV degradation results in the accumulation of multiple

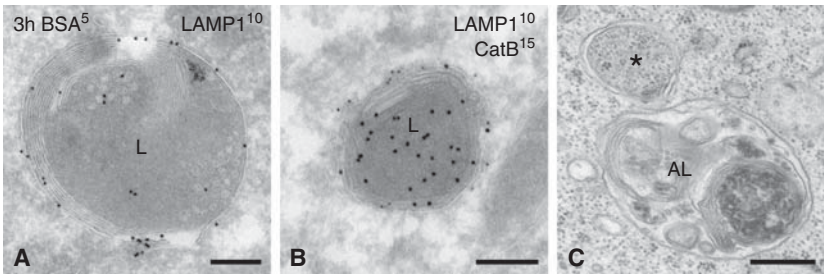


**Figure 4.** Picture gallery of lysosomes. (*A*) HepG2 cells pre-incubated for 3 h with BSA$^5$ and immunogold-labeled for LAMP1 (10-nm gold). Example of a typical lysosome with lamellar membranes, some ILVs, and an overall electron-dense content. LAMP1 is mainly restricted to the limiting membrane. (*B*) Another example from a HepG2 cell, showing the presence of lysosomal enzyme cathepsin B (CatB) (15-nm gold) in the electron-dense lumen and LAMP1 (10-nm gold) at the limiting membrane. (*C*) Autophagic compartments in a stimulated B cell. The asterisk points to a double-membrane vesicle sequestering the cytosol. The autolysosome (AL) contains more heterogeneous content than a regular lysosome. Techniques used: (*A*,*B*) chemical fixation and ultrathin cryosectioning; (*C*) chemical fixation and EPON embedding. Scale bar, 200 nm.

concentric membrane sheets within so-called lamellar lysosomes. Lamellar lysosomes are also particularly present in specialized immune cells containing specialized lysosomes involved in MHCII presentation, so-called MHC class II compartments (MIICs). MIICs are similar to "conventional" endosomes/lysosomes in terms of pH, accessibility by the endocytic pathway, and their composition of lysosomal proteins (Kleijmeer et al. 1997). ET reconstructions of HPF-fixed DCs and B lymphocytes, showed that the lamellae in MIICs are not connected to each other or the outer lysosomal membrane (Murk et al. 2004), but organized like the peel of an onion with membranes assembled on top of each other (Murk et al. 2004). How they are formed and assembled is unknown.

In some conditions, the spherically shaped lysosomes can become tubular. It is long known that MIICs become tubular in response to stimuli such as lipopolysaccharide (LPS) or the presence of T cells (Kleijmeer et al. 2001a; Chow et al. 2002), as part of the process to transfer peptide-loaded MHCII to the plasma membrane (Kleijmeer et al. 2001a). Tubular lysosomes have also been observed in other cell types, especially macrophages (Swanson et al. 1987). *Salmonella* infection induces formation of the *Salmonella*-containing vacuole (SCV) in the host cell, from which tubular, LAMP1-positive endolysosomes extend (Kaniuk et al. 2011; Cossart and Helenius 2014). Upon prolonged starvation, when nutrient levels are restored by the autophagy process (Yu et al. 2010; Rong et al. 2011), autolysosomes form tubules that by IEM are positive for LAMP1, but lack discernible luminal content or lysosomal enzymes (Yu et al. 2010). The luminal content remains behind in the autolysosomal vacuole while the LAMP1 tubules receive lysosomal enzymes and mature into functional lysosomes.

### Molecular Machinery Involved in Lysosome Tubulation

The spherical-to-tubular morphogenetic changes of the lysosomes serve to fulfill a particular function. How these structural changes are imposed and the machineries involved—other than a requirement for microtubules—are just beginning to be understood. Interestingly, studies in macrophages and *Salmonella*-infected cells both revealed a role for the Arf-like (Arl) lysosomal GTPase Arl8b (Kaniuk et al. 2011; Mrakovic et al. 2012). A genome-wide RNAi screen on MHCII antigen presentation revealed a role for another Arl family member, ARL14/ARF7 (Paul et al. 2011), but a possible role of Arl8b is not excluded and is currently under investigation (J Neefjes, pers. comm.). Arl8b mediates kinesin-1 recruitment to the microtubules (Kaniuk et al. 2011), but also recruits the HOPS (homotypic fusion and vacuolar protein sorting) tethering complex to lysosomes (Garg et al. 2011), which is important for lysosomal fusion events (Pols et al. 2013). It is not yet clear whether these functions are somehow related.

## RECYCLING ENDOSOMES

The progressive maturation of the vacuolar SEs into LEs is tightly linked to the generation of tubules that emanate from the uncoated areas of the SE vacuole to recycle cargo to the plasma membrane, but also to mediate transport to the TGN, to lysosomes, and, when present, to lysosome-related organelles (LROs) (Taguchi 2013). An SE vacuole can contain two to seven tubules, which frequently show bifurcations (Marbet et al. 2006). Fission of these tubules to form an RE triggers maturation of the SE vacuole (Mesaki et al. 2011). In some cells, such as CHO (Yamashiro et al. 1984), a collection of RE tubules can form the so-called endosomal recycling compartment (ERC), which defines a TfR-containing, juxtanuclear tubular network. In other cells (some HeLa cell clones, melanocytes), the REs remain more peripherally distributed (Delevoye et al. 2009) without forming a clearly distinguishable ERC. Cargoes undergo recycling to the plasma membrane by fast or slow kinetics, as described, for example, for Tf and its receptor (Maxfield and McGraw 2004; Grant and Donaldson 2009). The fast pathway is thought to operate directly from the tubules emerging from the SEs, whereas the slow-recycling pathway is thought to involve passage through the ERC or peripheral REs.

The ultrastructural complexity of the tubular networks formed by REs mirrors that of the TGN, the other crucial sorting station in the cell (Klumperman 2011). The tubules of ~60–100 nm in diameter (Willingham et al. 1984) extend along microtubules (Marsh et al. 1986) over long distances (up to 4 μm in length), even when still attached to an SE vacuole. Membrane continuities are difficult to appreciate on ultrathin sections but well resolved by ET (Delevoye et al. 2009). The complex network formed by RE tubules has also been visualized using whole-mount EM (Stoorvogel et al. 1996) highlighting the presence of clathrin-coated buds (as detailed below) of 60–80 nm in diameter, which is significantly smaller then the coated buds present at the TGN (100–110 nm).

Comprehending the structure/function relationship of REs was greatly furthered through visualization—by IF, but essentially IEM—of model cargo molecules: Tf, TfR, TGN38, furin, the insulin-regulated amino peptidase (IRAP), the glucose transporter (Glut4), G-protein-coupled receptors, and also lipids using fluorescent lipid analogs such as (C6-NBD-sphingomyelin) and toxins that bind glycolipids (e.g., B fragment of Shiga toxin) (for review, see Taguchi 2013). For example, in the human liver cell HepG2, a particular RE tubule was shown to contain the recycling proteins Tf and ASGPR, the lysosomal enzyme receptors CD and CI-MPR, and the lysosomal membrane proteins LAMP-1 and LAMP-2 (Peden et al. 2004). In addition, Tf and the B-fragment of Shiga toxin, destined for the plasma membrane and TGN, respectively, were found in the same RE tubule (Popoff et al. 2007). These observations suggest that REs in addition to SEs have a sorting function by concentrating cargoes into specified regions that recruit different machineries (Bonifacino and Rojas 2006). This led to the concept of the tubular sorting endosome (TSE) (Peden et al. 2004) or tubular endosomal network (TEN) (Bonifacino and Rojas 2006). The TSE/TEN concept implies that the protein machinery involved in cargo sorting (e.g., the sorting nexin family) (see Burd and Cullen 2014) can define various exit domains on RE tubules with different cellular fates (Bonifacino and Rojas 2006). In addition, distinct types of tubules can derive directly from an SE vacuole (Fig. 2).

## Coated Buds on REs

Clathrin-coated buds on endosomes bear the heterotetrameric adaptor complexes AP1 or AP3 (Stoorvogel et al. 1996; Dell'Angelica et al. 1998; Peden et al. 2004; Theos et al. 2005). AP1 buds accumulate cargoes that interact with this adaptor via di-leucine signals (Bonifacino and Traub 2003) but also cargoes such as TfR that do not bear particular sorting signals. AP1 on endosomal tubules has been implicated in the retrograde transport of MPRs and the Shiga toxin B subunit to the TGN (Mallard et al. 1998; Meyer et al. 2001; Hirst et al. 2012) and transport of the melanosomal protein TYRP1 to the melanosome, an LRO (Theos et al. 2005; Delevoye et al. 2009). AP1 could also be involved in recycling of internalized Tf to the plasma membrane (Mallard et al. 1998; van Dam and Stoorvogel 2002) even if this trafficking also occurs by default, independent of cytoplasmic sorting signals (for review, see Huotari and Helenius 2011). In polarized cells, TfR endocytosed from the basolateral membrane is actively sorted away from the default transcytotic pathway to the apical membrane and efficiently recycled to the basolateral plasma membrane via AP1B-coated buds (Futter et al. 1998; Folsch et al. 2001).

The adaptor AP3 is also associated with endosomal buds (Peden et al. 2004; Theos et al. 2005). AP3 has been implicated in the transport of lysosomal proteins from these RE tubules to lysosomes and of melanosomal proteins to melanosomes. Both types of buds, AP1 or AP3, have been observed within one contiguous tubule (Peden et al. 2004; Theos et al. 2005), illustrating the proposed sorting capacity of RE tubules. Depending on the interactions of the different cargoes with the different adaptors, sorting could occur concomitantly or sequentially for different destinations. Studies in melanocytic cells in which some cargoes interact with both adaptors or only one adaptor led to the proposal that the adaptors could act sequentially. For example, tyrosinase interacts with

AP3 and AP1 (Theos et al. 2005). This key enzyme in melanin synthesis is optimally sorted by AP3 but, in its absence, accumulates in AP1-coated buds and is still transported to the melanosome (Theos et al. 2005). Another melanosomal enzyme, TYRP1, that acts subsequently in melanin synthesis does not interact with AP3 and is sorted only by AP1 to the melanosome (Theos et al. 2005; Chapuy et al. 2008).

### RE Machinery Proteins

The generation and transport of RE tubules requires several machineries that act in a coordinated manner. Among these are Rab GTPases (Soennichsen et al. 2000; Stenmark 2009; Pfeffer 2013) involved in the maintenance of specialized membrane domains, sorting nexins (SNXs), and EHD proteins that are involved in membrane curvature and stabilization of tubules (Carlton and Cullen 2005; Cullen and Korswagen 2012), and also cytoskeletal elements, actin, microtubules, associated protein complexes, and motors required for imposing membrane tension, elongation of tubules, scission, and transport (Grant and Donaldson 2009).

Impairment of the function of any of these machineries impacts the recycling of cargoes, but generally the impairment is only partial. The partial inhibition observed when inactivating a particular pathway can certainly be explained by a redundancy of available pathways for a specific cargo, concomitant expression of isoforms of machinery proteins, or the multitude of components that act in a coordinated manner to regulate vesicular transport. Here we focus only on proteins that are known to contribute to the morphogenesis of REs.

### RAB GTPases

The dynamic relation between SEs and REs was followed in live cells using fluorescently tagged Rab5, Rab4, and Rab11 (Sonnichsen et al. 2000). Rab4 was found on both SEs and REs, suggesting that it may control the fast-recycling pathway for TfR (Van der Sluijs et al. 1992), and the β2 adrenergic receptor (β2-AR), a signaling GPCR that shuttles from SEs directly to the plasma membrane (Yudowski et al. 2009). Rab11 is mostly enriched in the juxtanuclear ERC or, depending on the cell type, peripheral RE domains (Ullrich et al. 1996) and regulates the slower-recycling pathway. Although REs are mainly defined by Rab4 (Van der Sluijs et al. 1992; Sheff et al. 1999) and Rab11 (Ullrich et al. 1996; Ren et al. 1998; Wilcke et al. 2000), additional Rab proteins (Rab17, Rab12, Rab14, Rab8, Rab10, Rab22A) also localize to REs (for review, see Grant and Donaldson 2009; Stenmark 2009; see also Wandinger-Ness and Zerial 2014). Because these Rab proteins share many common effectors, they likely mark overlapping membrane domains. The expression of a particular endosome-associated Rab protein may regulate the formation and maintenance of a given endosomal domain operating within a pathway for a particular cargo. Rabs and accessory proteins (different Rab isoforms, Rab effectors, protein complexes) are expressed at different levels in distinct cells to control different recycling pathways (Stenmark 2009). Interfering with the function of these GTPases highly impacts endosome morphology, which results either in impaired formation of tubules or, the opposite, extensive tubulation (Wilcke et al. 2000; Mesa et al. 2001). It would be of interest to investigate at the ultrastructural level the morphological features of each domain exploiting the particular localization of the Rabs.

## SORTING NEXINS AND THE WASH COMPLEX

Sorting nexins (SNXs) are a large family of proteins classified by the presence of a phosphoinositide-binding phox homology (PX) domain. For the SNX-BAR subgroup, the PX domain resides alongside a carboxy-terminal Bin/Amphiphysin/Rvs (BAR) domain (see Burd and Cullen 2014). Recent in vitro studies highlighted the membrane-remodeling properties of all 12 human SNX-BARs and revealed that only a selected number elicit the formation of tubules that resemble the RE tubules that emanate from the SE in vivo (van Weering et al. 2012). Different SNXs have been attributed to distinct recycling pathways emerging from SE vacuoles or

RE tubules (Cullen and Korswagen 2012). SNX1, SNX2, and possibly SNX5, SNX6 together with Vps26, Vps29, and Vps35a form a major heteropentameric complex called the retromer. The SNX1/2 dimer is required for endosomal membrane recruitment of the complex to Vps35a for cargo binding, including MPR, Wntless, and sortilin. SNX1/2 are involved in endosome-to-TGN transport as part of the retromer complex; SNX4 and SNX17 participate in cargo recycling from endosomes to the plasma membrane; and SNX8 in endosome-to-TGN trafficking in a retromer-independent manner. SNX27 is also involved in recycling to the plasma membrane and might act in a retromer-dependent or -independent manner. SNX27 has been recently shown to interact with the retromer subunit VPS26 via its PDZ domain, and such interaction is necessary and sufficient to prevent lysosomal entry of SNX27 cargo (such as, e.g., GLUT1, the copper transporter ATP7A) (Steinberg et al. 2013). On the other hand, studies on β2-AR revealed that SNX27 does not directly interact with the retromer core complex (VPS26, VPS29, and VPS35) but with the actin nucleation-promoting factor WASH (Wiskott–Aldrich syndrome protein and SCAR homolog) complex, which is associated with the retromer (Lauffer et al. 2010).

There is increasing evidence that the WASH complex, together with actin-related protein 2/3 (ARP2/3), is required for the integrity of endolysosomal compartments (Gomez et al. 2012). Because these actin-binding complexes associate with RE tubules they might control their initial formation, growth, and fission together with their associated cytoskeleton (Derivery et al. 2009; Duleh and Welch 2010; Seaman et al. 2013). Recent studies using live-cell imaging indicate that endosomal domains labeled with SNX1, SNX4, and SNX8 couple to discrete combinations of dynein and kinesin motors, which govern the structure and motility of each SNX-coated membrane as well as segregation of distinct functional endosomal subdomains (Hunt et al. 2013). If SNXs (but also so-called EHD proteins) (Naslavsky and Caplan 2011) are required for stabilization/curvature, the molecular motors (kinesins, dynein, and myosins) provide forces for pulling membranes, resulting in formation of tubules and their transport.

## MOLECULAR MOTORS

Various studies using conventional EM, IEM, or whole-mount EM have shown the presence of microtubules and actin in the vicinity of endosomes (Willingham and Pastan 1983; Parton et al. 1991; Tooze and Hollinshead 1991; Raposo et al. 1999; Salas-Cortes et al. 2005; Puthenveedu et al. 2010). Live-cell imaging enables visualization of events on single endosomes and revealed that the β2-AR is sorted to a subset of actin-rich RE tubules distinct from those containing TfR (Puthenveedu et al. 2010). Although the motors involved have not been identified, the actin associated with the cytosolic side of the tubules might be stabilized by the β2-AR because its carboxyl terminus interacts with actin-binding proteins such as ERM (Cao et al. 1999). In this particular case, it is unclear whether microtubule-dependent forces are required. For other cargoes the transport of RE/ERC intermediates to the cell surface need both actin and microtubules and their associated myosin and kinesin motors, respectively (Grant and Donaldson 2009). Myosin Vb associates with the ERC by interacting with RAB11 (Lapierre and Goldenring 2005), and MyosinIB associates with tubules emerging from SE vacuoles (Salas-Cortes et al. 2005). Such interactions certainly provide forces for membrane deformation and curvature (a model that parallels the one proposed for tubule formation at the TGN by unconventional and conventional Myosin II) (Miserey-Lenkei et al. 2010; Almeida et al. 2011).

Membrane deformation by actin and myosins is, in most cases, coupled to microtubule-dependent transport that allows transport over longer ranges; but how the two cytoskeletal systems are coordinated is still unclear. The motors required for the initial generation of the RE tubular network are still to be identified. KIF16B is associated with SEs and regulates their motility in a Rab5-dependent manner (Hoepfner et al. 2005). KIF3B has been implicated in the sorting of Tf/TfR from the ERC via an interac-

tion with the Rab11-binding protein Rip11 (FIP5) (Schonteich et al. 2008). Studies in melanocytic cells showed that KIF13A is a good candidate to participate in the initial generation of RE tubules from SEs. This kinesin interacts with the adaptor AP1 (Nakagawa et al. 2000; Delevoye et al. 2009), and this interaction is responsible for the extension of RE tubules from SEs and their transport to the cell periphery, in particular, in melanocytes, in close proximity to melanosomes (Delevoye et al. 2009, 2014). These results revealed that the morphogenesis of REs and their transport can be tightly coordinated with sorting by means of direct interactions with adaptors and cargoes.

## CONCLUDING REMARKS AND FUTURE PERSPECTIVES

The combination of imaging methods and recent developments of these techniques (super-resolution microscopy, CLEM, and 3D-ET) has provided a general view of the dynamic and complex organization of the endolysosomal system. Because many components coordinate in space and time to generate the different endolysosomal intermediates, it would be useful for our general understanding to better decipher the fine details, for example, to optimize the detection of components associated with different membrane subdomains and to investigate how a particular cargo influences the creation of a trafficking intermediate and its fate. Studies of particular processes such as cytokinesis and cilia formation have started to shed light on how the endosomal system can be diverted from its endocytic ubiquitous function (Montagnac and Chavrier 2008; Westlake et al. 2011). In addition, analyses of specialized cells, for example, distinct types of immune cells (B lymphocytes, dendritic cells, Langerhans cells, cytotoxic T cells) or skin cells (melanocytes), but also polarized epithelial cells, are interesting models to further enlighten the complex organization and ultrastructure of the endolysosomal system. From these studies, it is now well appreciated that the endosomal organization of one cell type cannot always be simply transferred to others. For example, components that are localized to LEs and lysosomes in most cells (e.g., CD63) are mostly enriched in LROs in melanocytes, platelets, and other LRO-containing cells (Marks et al. 2013). An additional example is Rab11/STX13-positive REs that in specialized cells are diverted from their ubiquitous recycling function to the plasma membrane for transport to LROs (Menager et al. 2007; Delevoye et al. 2009). In some instances, these REs, by retention of particular cargoes, can accommodate to become novel organelles as exemplified by the generation of Birbeck granules (McDermott et al. 2002). Thus, these cells adapt ubiquitous endosomal pathways to facilitate regulated cargo sorting and create novel organelles with specialized functions. How these pathways are exploited at the molecular level is still unclear, but may require a fine-tuning of the interactions between components of known pathways as well as the involvement of additional machineries that impact selected pathways.

## ACKNOWLEDGMENTS

We thank our many colleagues who have contributed to the work described herein, particularly Viola Oorschot and Guillaume van Niel for contributing figures. We apologize to those whose work we failed to cite. We are grateful for funding from the Netherlands Organization for Scientific Research (NWO) (VICI grant 918.56.611), the National Institutes of Health (grant R01 EY015625), Institute Curie, CNRS, and Foundation ARC pour la recherche sur le cancer (grant SL220100601359).

## REFERENCES

*Reference is also in this collection.

Allen RD, Fok AK. 1980. Membrane recycling and endocytosis in *Paramecium* confirmed by horseradish peroxidase pulse-chase studies. *J Cell Sci* **45:** 131–145.

Almeida CG, Yamada A, Tenza D, Louvard D, Raposo G, Coudrier E. 2011. Myosin 1b promotes the formation of post-Golgi carriers by regulating actin assembly and membrane remodelling at the *trans*-Golgi network. *Nat Cell Biol* **13:** 779–789.

Anderson RGW, Falck JR, Goldstein JL, Brown MS. 1984. Visualization of acidic organelles in intact cells by electron microscopy. *Proc Natl Acad Sci* **81:** 4838–4842.

Babst M, Wendland B, Estepa EJ, Emr SD. 1998. The Vps4p AAA ATPase regulates membrane association of a Vps protein complex required for normal endosome function. *EMBO J* **17:** 2982–2993.

Bainton DF. 1981. The discovery of lysosomes. *J Cell Biol* **91:** 66s–76s.

Bhisey AN, Freed JJ. 1971. Altered movement of endosomes in colchicine-treated cultured macrophages. *Exp Cell Res* **64:** 430–438.

* Bissig C, Gruenberg J. 2013. Lipid sorting and multivesicular endosome biogenesis. *Cold Spring Harb Perspect Biol* **5:** a016816.

Bonifacino JS, Rojas R. 2006. Retrograde transport from endosomes to the *trans*-Golgi network. *Nat Rev Mol Cell Biol* **7:** 568–579.

Bonifacino JS, Traub LM. 2003. Signals for sorting of transmembrane proteins to endosomes and lysosomes. *Annu Rev Biochem* **72:** 395–447.

Bright NA, Lindsay MR, Stewart A, Luzio JP. 2001. The relationship between lumenal and limiting membranes in swollen late endocytic compartments formed after wortmannin treatment or sucrose accumulation. *Traffic* **2:** 631–642.

Bright NA, Gratian MJ, Luzio JP. 2005. Endocytic delivery to lysosomes mediated by concurrent fusion and kissing events in living cells. *Curr Biol* **15:** 360–365.

* Burd C, Cullen PJ. 2014. Retromer: A master conductor of endosome sorting. *Cold Spring Harb Perspect Biol* doi: 10.1101/cshperspect.a016774.

Buschow SI, Nolte-'t Hoen EN, van Niel G, Pols MS, ten Broeke T, Lauwen M, Ossendorp F, Melief CJ, Raposo G, Wubbolts R, et al. 2009. MHC II in dendritic cells is targeted to lysosomes or T cell–induced exosomes via distinct multivesicular body pathways. *Traffic* **10:** 1528–1542.

Cao TT, Deacon HW, Reczek D, Bretscher A, von Zastrow M. 1999. A kinase-regulated PDZ-domain interaction controls endocytic sorting of the β2-adrenergic receptor. *Nature* **401:** 286–290.

Carlton JG, Cullen PJ. 2005. Sorting nexins. *Curr Biol* **15:** R819–R820.

Chapuy B, Tikkanen R, Muhlhausen C, Wenzel D, von Figura K, Honing S. 2008. AP-1 and AP-3 mediate sorting of melanosomal and lysosomal membrane proteins into distinct post-Golgi trafficking pathways. *Traffic* **9:** 1157–1172.

Chow A, Toomre D, Garrett W, Mellman I. 2002. Dendritic cell maturation triggers retrograde MHC class II transport from lysosomes to the plasma membrane. *Nature* **418:** 988–994.

* Cossart P, Helenius A. 2014. Endocytosis of viruses and bacteria. *Cold Spring Harb Perspect Biol* doi: 10.1101/cshperspect.a016972.

Cullen PJ, Korswagen HC. 2012. Sorting nexins provide diversity for retromer-dependent trafficking events. *Nat Cell Biol* **14:** 29–37.

Delevoye C, Hurbain I, Tenza D, Sibarita JB, Uzan-Gafsou S, Ohno H, Geerts WJ, Verkleij AJ, Salamero J, Marks MS, et al. 2009. AP-1 and KIF13A coordinate endosomal sorting and positioning during melanosome biogenesis. *J Cell Biol* **187:** 247–264.

Delevoye C, Miserey-Lenkei S, Montagnac G, Gilles-Marsens F, Paul Gilloteaux P, Giordano F, Waharte F, Marks MS, Goud B, Raposo G. 2014. Recycling endosome tubule morphogenesis from sorting endosomes requires the kinesin motor KIF13A. *Cell Rep* **6:** 1–10.

Dell'Angelica EC, Klumperman J, Stoorvogel W, Bonifacino JS. 1998. Association of the AP-3 adaptor complex with clathrin. *Science* **280:** 431–434.

De Maziere AM, Muehlethaler K, Van Donselaar E, Salvi S, Davoust J, Cerottini JC, Levy F, Slot JW, Rimoldi D. 2002. The melanocytic protein Melan-A/MART-1 has a subcellular localization distinct from typical melanosomal proteins. *Traffic* **3:** 678–693.

Derivery E, Sousa C, Gautier JJ, Lombard B, Loew D, Gautreau A. 2009. The Arp2/3 activator WASH controls the fission of endosomes through a large multiprotein complex. *Dev Cell* **17:** 712–723.

Duleh SN, Welch MD. 2010. WASH and the Arp2/3 complex regulate endosome shape and trafficking. *Cytoskeleton* **67:** 193–206.

Eden ER, White IJ, Tsapara A, Futter CE. 2010. Membrane contacts between endosomes and ER provide sites for PTP1B–epidermal growth factor receptor interaction. *Nat Cell Biol* **12:** 267–272.

Eskelinen EL, Reggiori F, Baba M, Kovacs AL, Seglen PO. 2011. Seeing is believing: The impact of electron microscopy on autophagy research. *Autophagy* **7:** 935–956.

Folsch H, Pypaert M, Schu P, Mellman I. 2001. Distribution and function of AP-1 clathrin adaptor complexes in polarized epithelial cells. *J Cell Biol* **152:** 595–606.

Friedman JR, DiBenedetto JR, West M, Rowland AA, Voeltz GK. 2013. Endoplasmic reticulum–endosome contact increases as endosomes traffic and mature. *Mol Biol Cell* **24:** 1030–1040.

Futter CE, Pearse A, Hewlett LJ, Hopkins CR. 1996. Multivesicular endosomes containing internalized EGF–EGF receptor complexes mature and then fuse directly with lysosomes. *J Cell Biol* **132:** 1011–1023.

Futter CE, Gibson A, Allchin EH, Maxwell S, Ruddock LJ, Odorizzi G, Domingo D, Trowbridge IS, Hopkins CR. 1998. In polarized MDCK cells basolateral vesicles arise from clathrin-γ-adaptin-coated domains on endosomal tubules. *J Cell Biol* **141:** 611–623.

Futter CE, Collinson LM, Backer JM, Hopkins CR. 2001. Human VPS34 is required for internal vesicle formation within multivesicular endosomes. *J Cell Biol* **155:** 1251–1264.

Garg S, Sharma M, Ung C, Tuli A, Barral DC, Hava DL, Veerapen N, Besra GS, Hacohen N, Brenner MB. 2011. Lysosomal trafficking, antigen presentation, and microbial killing are controlled by the Arf-like GTPase Arl8b. *Immunity* **35:** 182–193.

Geuze HJ, Slot JW, Scheffer RCT, Van der Ley PA. 1981. Use of colloidal gold particles in double-labeling immunoelectron microscopy of ultrathin frozen tissue sections. *J Cell Biol* **89:** 653–665.

Geuze HJ, Slot JW, Strous GJ, Lodish HF, Schwartz AL. 1983. Intracellular site of asialoglycoprotein receptor-ligand uncoupling: Double label immunoelectron microscopy during receptor-mediated endocytosis. *Cell* **32:** 277–287.

Giordano F, Simoes S, Raposo G. 2011. The ocular albinism type 1 (OA1) GPCR is ubiquitinated and its traffic requires endosomal sorting complex responsible for transport (ESCRT) function. *Proc Natl Acad Sci* **108:** 11906–11911.

Gomez TS, Gorman JA, de Narvajas AA, Koenig AO, Billadeau DD. 2012. Trafficking defects in WASH-knockout fibroblasts originate from collapsed endosomal and lysosomal networks. *Mol Biol Cell* **23:** 3215–3228.

Gonatas NK, Kim SU, Stieber A, Avrameas S. 1977. Internalization of lectins in neuronal GERL. *J Cell Biol* **73:** 1–13.

Gorvel JP, Chavrier P, Zerial M, Gruenberg J. 1991. rab5 Controls early endosome fusion in vitro. *Cell* **64:** 915–925.

Goud B, Legrain P, Antoine JC, Avrameas S, Buttin G. 1981. Cross-linking of surface immunoglobulins and endocytosis of antigen are not sufficient to suppress antibody production of two hybridoma cell lines. *J Recept Res* **2:** 63–85.

Gould GW, Lippincott-Schwartz J. 2009. New roles for endosomes: From vesicular carriers to multi-purpose platforms. *Nat Rev Mol Cell Biol* **10:** 287–292.

Grant BD, Donaldson JG. 2009. Pathways and mechanisms of endocytic recycling. *Nat Rev Mol Cell Biol* **10:** 597–608.

Griffiths G. 1993. *Fine structure immunocytochemistry.* Springer, New York.

Gruenberg J, Stenmark H. 2004. The biogenesis of multivesicular endosomes. *Nat Rev Mol Cell Biol* **5:** 317–323.

Hanson PI, Cashikar A. 2012. Multivesicular body morphogenesis. *Ann Rev Cell Dev Biol* **28:** 337–362.

Hawes P, Netherton CL, Mueller M, Wileman T, Monaghan P. 2007. Rapid freeze-substitution preserves membranes in high-pressure frozen tissue culture cells. *J Microsc* **226:** 182–189.

* Henne WM, Stenmark H, Emr SD. 2013. Molecular mechanisms of the membrane sculpting ESCRT pathway. *Cold Spring Harb Perspect Biol* **5:** a016766.

Hirst J, Borner GH, Antrobus R, Peden AA, Hodson NA, Sahlender DA, Robinson MS. 2012. Distinct and overlapping roles for AP-1 and GGAs revealed by the "knocksideways" system. *Curr Biol* **22:** 1711–1716.

Hoepfner S, Severin F, Cabezas A, Habermann B, Runge A, Gillooly D, Stenmark H, Zerial M. 2005. Modulation of receptor recycling and degradation by the endosomal kinesin KIF16B. *Cell* **121:** 437–450.

Hunt SD, Townley AK, Danson CM, Cullen PJ, Stephens DJ. 2013. Microtubule motors mediate endosomal sorting by maintaining functional domain organization. *J Cell Sci* **126:** 2493–2501.

Huotari J, Helenius A. 2011. Endosome maturation. *EMBO J* **30:** 3481–3500.

Hurbain I, Geerts WJ, Boudier T, Marco S, Verkleij AJ, Marks MS, Raposo G. 2008. Electron tomography of early melanosomes: Implications for melanogenesis and the generation of fibrillar amyloid sheets. *Proc Natl Acad Sci* **105:** 19726–19731.

Johansson M, Rocha N, Zwart W, Jordens I, Janssen L, Kuijl C, Olkkonen VM, Neefjes J. 2007. Activation of endosomal dynein motors by stepwise assembly of Rab7–RILP–p150$^{Glued}$, ORP1L, and the receptor βIII spectrin. *J Cell Biol* **176:** 459–471.

Jordens I, Fernandez-Borja M, Marsman M, Dusseljee S, Janssen L, Calafat J, Janssen H, Wubbolts R, Neefjes J. 2001. The Rab7 effector protein RILP controls lysosomal transport by inducing the recruitment of dynein-dynactin motors. *Curr Biol* **11:** 1680–1685.

Kaniuk NA, Canadien V, Bagshaw RD, Bakowski M, Braun V, Landekic M, Mitra S, Huang J, Heo WD, Meyer T, et al. 2011. *Salmonella* exploits Arl8B-directed kinesin activity to promote endosome tubulation and cell-to-cell transfer. *Cell Microbiol* **13:** 1812–1823.

Kleijmeer MJ, Morkowski S, Griffith JM, Rudensky AY, Geuze HJ. 1997. Major histocompatibility complex class II compartments in human and mouse B lymphoblasts represent conventional endocytic compartments. *J Cell Biol* **139:** 639–649.

Kleijmeer M, Ramm G, Schuurhuis D, Griffith J, Rescigno M, Ricciardi-Castagnoli P, Rudensky AY, Ossendorp F, Melief CJ, Stoorvogel W, et al. 2001a. Reorganization of multivesicular bodies regulates MHC class II antigen presentation by dendritic cells. *J Cell Biol* **155:** 53–63.

Kleijmeer MJ, Escola JM, UytdeHaag FG, Jakobson E, Griffith JM, Osterhaus AD, Stoorvogel W, Melief CJ, Rabouille C, Geuze HJ. 2001b. Antigen loading of MHC class I molecules in the endocytic tract. *Traffic* **2:** 124–137.

Klumperman J. 2011. Architecture of the mammalian Golgi. *Cold Spring Harb Perspect Biol* **3:** a005181.

Kobayashi T, Stang E, Fang KS, de Moerloose P, Parton RG, Gruenberg J. 1998. A lipid associated with the antiphospholipid syndrome regulates endosome structure and function. *Nature* **392:** 193–197.

Kolter T, Sandhoff K. 2010. Lysosomal degradation of membrane lipids. *FEBS Lett* **584:** 1700–1712.

Konig P, Braunfeld MB, Sedat JW, Agard DA. 2007. The three-dimensional structure of in vitro reconstituted *Xenopus laevis* chromosomes by EM tomography. *Chromosoma* **116:** 349–372.

Koster AJ, Klumperman J. 2003. Electron microscopy in cell biology: Integrating structure and function. *Nat Rev Mol Cell Biol* SS6–S10.

Kukulski W, Schorb M, Kaksonen M, Briggs JA. 2012a. Plasma membrane reshaping during endocytosis is revealed by time-resolved electron tomography. *Cell* **150:** 508–520.

Kukulski W, Schorb M, Welsch S, Picco A, Kaksonen M, Briggs JA. 2012b. Precise, correlated fluorescence microscopy and electron tomography of lowicryl sections using fluorescent fiducial markers. *Method Cell Biol* **111:** 235–257.

Lapierre LA, Goldenring JR. 2005. Interactions of Myosin Vb with Rab11 family members and cargoes traversing the plasma membrane recycling system. *Method Enzymol* **403:** 715–723.

Lauffer BE, Melero C, Temkin P, Lei C, Hong W, Kortemme T, von Zastrow M. 2010. SNX27 mediates PDZ-directed sorting from endosomes to the plasma membrane. *J Cell Biol* **190:** 565–574.

Louvard D, Morris C, Warren G, Stanley K, Winkler F, Reggio H. 1983. A monoclonal antibody to the heavy chain of clathrin. *EMBO J* **2:** 1655–1664.

Luzio JP, Gray SR, Bright NA. 2010. Endosome–lysosome fusion. *Biochem Soc Trans* **38:** 1413–1416.

Mallard F, Antony C, Tenza D, Salamero J, Goud B, Johannes L. 1998. Direct pathway from early/recycling endosomes to the Golgi apparatus revealed through the study of Shiga toxin B-fragment transport. *J Cell Biol* **143:** 973–990.

Marbet P, Rahner C, Stieger B, Landmann L. 2006. Quantitative microscopy reveals 3D organization and kinetics of endocytosis in rat hepatocytes. *Microsc Res Tech* **69:** 693–707.

Mari M, Bujny MV, Zeuschner D, Geerts WJ, Griffith J, Petersen CM, Cullen PJ, Klumperman J, Geuze HJ. 2008. SNX1 defines an early endosomal recycling exit for sortilin and mannose 6-phosphate receptors. *Traffic* **9:** 380–393.

Marks MS, Heijnen HF, Raposo G. 2013. Lysosome-related organelles: Unusual compartments become mainstream. *Curr Opin Cell Biol* **25:** 495–505.

Marsh M, Griffiths G, Dean GE, Mellman I, Helenius A. 1986. Three-dimensional structure of endosomes in BHK-21 cells. *Proc Natl Acad Sci* **83:** 2899–2903.

Matsuo H, Chevallier J, Mayran N, Le Blanc I, Ferguson C, Faure J, Blanc NS, Matile S, Dubochet J, Sadoul R, et al. 2004. Role of LBPA and Alix in multivesicular liposome formation and endosome organization. *Science* **303:** 531–534.

* Maxfield FR. 2014. Role of endosomes and lysosomes in human disease. *Cold Spring Harb Perspect Biol* doi: 10.1101/cshperspect.a016931.

Maxfield FR, McGraw TE. 2004. Endocytic recycling. *Nat Rev Mol Cell Biol* **5:** 121–132.

Mayor S, Pagano RE. 2007. Pathways of clathrin-independent endocytosis. *Nat Rev Mol Cell Biol* **8:** 603–612.

* Mayor S, Parton RG, Donaldson JG. 2014. Clathrin-independent pathways of endocytosis. *Cold Spring Harb Perspect Biol* doi: 10.1101/cshperspect.a016758.

McDermott R, Ziylan U, Spehner D, Bausinger H, Lipsker D, Mommaas M, Cazenave JP, Raposo G, Goud B, de la Salle H, et al. 2002. Birbeck granules are subdomains of endosomal recycling compartment in human epidermal Langerhans cells, which form where Langerin accumulates. *Mol Biol Cell* **13:** 317–335.

Menager MM, Menasche G, Romao M, Knapnougel P, Ho CH, Garfa M, Raposo G, Feldmann J, Fischer A, de Saint Basile G. 2007. Secretory cytotoxic granule maturation and exocytosis require the effector protein hMunc13-4. *Nat Immunol* **8:** 257–267.

Mesa R, Salomon C, Roggero M, Stahl PD, Mayorga LS. 2001. Rab22a affects the morphology and function of the endocytic pathway. *J Cell Sci* **114:** 4041–4049.

Mesaki K, Tanabe K, Obayashi M, Oe N, Takei K. 2011. Fission of tubular endosomes triggers endosomal acidification and movement. *PLoS ONE* **6:** e19764.

Meyer C, Eskelinen EL, Guruprasad MR, von Figura K, Schu P. 2001. Mu 1A deficiency induces a profound increase in MPR300/IGF-II receptor internalization rate. *J Cell Sci* **114:** 4469–4476.

Mironov AA, Beznoussenko GV. 2012. Correlative light-electron microscopy a potent tool for the imaging of rare or unique cellular and tissue events and structures. *Methods Enzymol* **504:** 201–219.

Miserey-Lenkei S, Chalancon G, Bardin S, Formstecher E, Goud B, Echard A. 2010. Rab and actomyosin-dependent fission of transport vesicles at the Golgi complex. *Nat Cell Biol* **12:** 645–654.

Möbius W, Ohno-Iwashita Y, van Donselaar EG, Oorschot VM, Shimada Y, Fujimoto T, Heijnen HF, Geuze HJ, Slot JW. 2002. Immunoelectron microscopic localization of cholesterol using biotinylated and non-cytolytic perfringolysin O. *J Histochem Cytochem* **50:** 43–55.

Möbius W, van Donselaar E, Ohno-Iwashita Y, Shimada Y, Heijnen HF, Slot JW, Geuze HJ. 2003. Recycling compartments and the internal vesicles of multivesicular bodies harbor most of the cholesterol found in the endocytic pathway. *Traffic* **4:** 222–231.

Montagnac G, Chavrier P. 2008. Endosome positioning during cytokinesis. *Biochem Soc Trans* **36:** 442–443.

Mrakovic A, Kay JG, Furuya W, Brumell JH, Botelho RJ. 2012. Rab7 and Arl8 GTPases are necessary for lysosome tubulation in macrophages. *Traffic* **13:** 1667–1679.

Muller-Reichert T, Verkade P. 2012. Introduction to correlative light and electron microscopy. *Method Cell Biol* **111:** xvii–xix.

Muller-Reichert T, Hohenberg H, O'Toole ET, McDonald K. 2003. Cryoimmobilization and three-dimensional visualization of *C. elegans* ultrastructure. *J Microsc* **212:** 71–80.

Mullock BM, Bright NA, Fearon CW, Gray SR, Luzio JP. 1998. Fusion of lysosomes with late endosomes produces a hybrid organelle of intermediate density and is NSF dependent. *J Cell Biol* **140:** 591–601.

Murk J, Humbel BM, Zlese U, Griffith J, Posthuma G, Slot JW, Koster A, Verkleij H, Geuze H, Kleijmeer MJ. 2003a. Endosomal comparttimentalization in three dimensions: Implications for membrane fusion. *Proc Natl Acad Sci* **100:** 13332–13337.

Murk JL, Posthuma G, Koster AJ, Geuze HJ, Verkleij AJ, Kleijmeer MJ, Humbel BM. 2003b. Influence of aldehyde fixation on the morphology of endosomes and lysosomes: Quantitative analysis and electron tomography. *J Microsc* **212:** 81–90.

Murk JL, Lebbink MN, Humbel BM, Geerts WJ, Griffith JM, Langenberg DM, Verreck FA, Verkleij AJ, Koster AJ, Geuze HJ, Kleijmeer MJ. 2004. 3-D Structure of multilaminar lysosomes in antigen presenting cells reveals trapping of MHC II on the internal membranes. *Traffic* **12:** 936–945.

Nakagawa T, Setou M, Seog D, Ogasawara K, Dohmae N, Takio K, Hirokawa N. 2000. A novel motor, KIF13A, transports mannose-6-phosphate receptor to plasma membrane through direct interaction with AP-1 complex. *Cell* **103:** 569–581.

Naslavsky N, Caplan S. 2011. EHD proteins: Key conductors of endocytic transport. *Trend Cell Biol* **21:** 122–131.

Novikoff AB, Novikoff PM. 1977. Cytochemical contributions to differentiating GERL from the Golgi apparatus. *Histochem J* **9:** 525–551.

Novikoff AB, Beaufay H, De Duve C. 1956. Electron microscopy of lysosomerich fractions from rat liver. *J Biophys Biochem Cytol* **2:** 179–184.

Odorizzi G, Babst M, Emr SD. 1998. Fab1p PtdIns(3)P 5-kinase function essential for protein sorting in the multivesicular body. *Cell* **95:** 847–858.

Parton RG, Dotti CG, Bacallao R, Kurtz I, Simons K, Prydz K. 1991. pH-induced microtubule-dependent redistribution of late endosomes in neuronal and epithelial cells. *J Cell Biol* **113:** 261–274.

Paul P, van den Hoorn T, Jongsma ML, Bakker MJ, Hengeveld R, Janssen L, Cresswell P, Egan DA, van Ham M, Ten Brinke A, et al. 2011. A genome-wide multidimensional RNAi screen reveals pathways controlling MHC class II antigen presentation. *Cell* **145:** 268–283.

Peden AA, Oorschot V, Hesser BA, Austin CD, Scheller RH, Klumperman J. 2004. Localization of the AP-3 adaptor complex defines a novel endosomal exit site for lysosomal membrane proteins. *J Cell Biol* **164:** 1065–1076.

Pfeffer SR. 2013. Rab GTPase regulation of membrane identity. *Curr Opin Cell Biol* **25:** 414–419.

Polishchuk RS, Polishchuk EV, Luini A. 2012. Visualizing live dynamics and ultrastructure of intracellular organelles with preembedding correlative light-electron microscopy. *Method Cell Biol* **111:** 21–35.

Pols MS, Klumperman J. 2009. Trafficking and function of the tetraspanin CD63. *Exp Cell Res* **315:** 1584–1592.

Pols MS, van Meel E, Oorschot V, ten Brink C, Fukuda M, Swetha MG, Mayor S, Klumperman J. 2013. hVps41 and VAMP7 function in direct TGN to late endosome transport of lysosomal membrane proteins. *Nat Commun* **4:** 1361.

Popoff V, Mardones GA, Tenza D, Rojas R, Lamaze C, Bonifacino JS, Raposo G, Johannes L. 2007. The retromer complex and clathrin define an early endosomal retrograde exit site. *J Cell Sci* **120:** 2022–2031.

Prekeris R, Klumperman J, Chen YA, Scheller RH. 1998. Syntaxin 13 mediates cycling of plasma membrane proteins via tubulovesicular recycling endosomes. *J Cell Biol* **143:** 957–971.

Puthenveedu MA, Lauffer B, Temkin P, Vistein R, Carlton P, Thorn K, Taunton J, Weiner OD, Parton RG, von Zastrow M. 2010. Sequence-dependent sorting of recycling proteins by actin-stabilized endosomal microdomains. *Cell* **143:** 761–773.

Raiborg C, Bache KG, Mehlum A, Stang E, Stenmark H. 2001. Hrs recruits clathrin to early endosomes. *EMBO J* **20:** 5008–5021.

Raiborg C, Bache KG, Gillooly DJ, Madshus IH, Stang E, Stenmark H. 2002. Hrs sorts ubiquitinated proteins into clathrin-coated microdomains of early endosomes. *Nat Cell Biol* **4:** 394–398.

Ranftler C, Auinger A, Meisslitzer-Ruppitsch C, Neumüller J, Ellinger A, Pavelka M. 2013. Electron microscopy of endocytic pathways. In *Cell imaging techniques: Methods and protocols*, 2nd ed. (ed. Taatjes DJ, Roth J), pp. 437–447. Humana, Totowa, NJ.

Raposo G, Stoorvogel W. 2013. Extracellular vesicles: Exosomes, microvesicles, and friends. *J Cell Biol* **200:** 373–383.

Raposo G, Kleijmeer MJ, Posthuma G, Slot JW, Geuze HJ. 1997. Immunogold labeling of ultrathin cryosections: Application in immunology. In *Weir's handbook of experimental immunology, immunochemistry and molecular immunology* (ed. Weir DM), Chap. 208, pp. 1–11. Wiley, New York.

Raposo G, Cordonnier MN, Tenza D, Menichi B, Durrbach A, Louvard D, Coudrier E. 1999. Association of myosin Iα with endosomes and lysosomes in mammalian cells. *Mol Biol Cell* **10:** 1477–1494.

Raposo G, Tenza D, Murphy DM, Berson JF, Marks MS. 2001. Distinct protein sorting and localization to premelanosomes, melanosomes, and lysosomes in pigmented melanocytic cells. *J Cell Biol* **152:** 809–824.

Ren M, Xu G, Zeng J, De Lemos-Chiarandini C, Adesnik M, Sabatini DD. 1998. Hydrolysis of GTP on Rab11 is required for the direct delivery of transferrin from the pericentriolar recycling compartment to the cell surface but not from sorting endosomes. *Proc Natl Acad Sci* **95:** 6187–6192.

Rink J, Ghigo E, Kalaidzidis Y, Zerial M. 2005. Rab conversion as a mechanism of progression from early to late endosomes. *Cell* **122:** 735–749.

Rocha N, Kuijl C, van der Kant R, Janssen L, Houben D, Janssen H, Zwart W, Neefjes J. 2009. Cholesterol sensor ORP1L contacts the ER protein VAP to control Rab7–RILP–p150$^{Glued}$ and late endosome positioning. *J Cell Biol* **185:** 1209–1225.

Rojas R, van Vlijmen T, Mardones GA, Prabhu Y, Rojas AL, Mohammed S, Heck AJ, Raposo G, van der Sluijs P, Bonifacino JS. 2008. Regulation of retromer recruitment to endosomes by sequential action of Rab5 and Rab7. *J Cell Biol* **183:** 513–526.

Romao M, Tanaka K, Sibarita JB, Ly-Hartig NT, Tanaka TU, Antony C. 2008. Three-dimensional electron microscopy analysis of ndc10-1 mutant reveals an aberrant organization of the mitotic spindle and spindle pole body defects in *Saccharomyces cerevisiae*. *J Struct Biol* **163:** 18–28.

Rong Y, McPhee CK, Deng S, Huang L, Chen L, Liu M, Tracy K, Baehrecke EH, Yu L, Lenardo MJ. 2011. Spinster is required for autophagic lysosome reformation and mTOR reactivation following starvation. *Proc Natl Acad Sci* **108:** 7826–7831.

Rybin V, Ullrich O, Rubino M, Alexandrov K, Simon I, Seabra MC, Goody R, Zerial M. 1996. GTPase activity of Rab5 acts as a timer for endocytic membrane fusion. *Nature* **383:** 266–269.

Sachse M, Ramm G, Strous G, Klumperman J. 2002a. Endosomes: Multipurpose designs for integrating housekeeping and specialized tasks. *Histochem Cell Biol* **117:** 91–104.

Sachse M, Urbe S, Oorschot V, Strous GJ, Klumperman J. 2002b. Bilayered clathrin coats on endosomal vacuoles are involved in protein sorting toward lysosomes. *Mol Biol Cell* **13:** 1313–1328.

Sachse M, Strous GJ, Klumperman J. 2004. ATPase-deficient hVPS4 impairs formation of internal endosomal vesicles and stabilizes bilayered clathrin coats on endosomal vacuoles. *J Cell Sci* **117:** 1699–1708.

Saftig P, Klumperman J. 2009. Lysosome biogenesis and lysosomal membrane proteins: Trafficking meets function. *Nat Rev Mol Cell Biol* **10:** 623–635.

Salas-Cortes L, Ye F, Tenza D, Wilhelm C, Theos A, Louvard D, Raposo G, Coudrier E. 2005. Myosin Ib modulates the morphology and the protein transport within multi-vesicular sorting endosomes. *J Cell Sci* **118:** 4823–4832.

Schonteich E, Wilson GM, Burden J, Hopkins CR, Anderson K, Goldenring JR, Prekeris R. 2008. The Rip11/Rab11-FIP5 and kinesin II complex regulates endocytic protein recycling. *J Cell Sci* **121:** 3824–3833.

Seaman MN, Gautreau A, Billadeau DD. 2013. Retromer-mediated endosomal protein sorting: All WASHed up! *Trend Cell Biol* **23:** 522–528.

Sheff DR, Daro EA, Hull M, Mellman I. 1999. The receptor recycling pathway contains two distinct populations of early endosomes with different sorting functions. *J Cell Biol* **145:** 123–139.

Shio H, Farquhar MG, de Duve C. 1974. Lysosomes of the arterial wall. IV. Cytochemical localization of acid phosphatase and catalase in smooth muscle cells and foam cells from rabbit atheromatous aorta. *Am J Pathol* **76:** 1–16.

Shu X, Lev-Ram V, Deerinck TJ, Qi Y, Ramko EB, Davidson MW, Jin Y, Ellisman MH, Tsien RY. 2011. A genetically encoded tag for correlated light and electron microscopy of intact cells, tissues, and organisms. *PLoS Biol* **9:** e1001041.

Slot JW, Geuze HJ. 1981. Sizing of protein A–colloidal gold probes for immunoelectron microscopy. *J Cell Biol* **90:** 533–536.

Slot JW, Geuze HJ. 2007. Cryosectioning and immunolabeling. *Nat Protoc* **2:** 2480–2491.

Slot JW, Posthuma G, Chang L, Crapo JD, Geuze HJ. 1988. Quantitative assessment of immuno-gold labeling in cryosections. In *Immuno-gold labeling in cell biology* (ed. Verleij AJ, Leunissen JLM), pp. 135–156. CRC, Boca Raton, FL.

Sonnichsen B, De Renzis S, Nielsen E, Rietdorf J, Zerial M. 2000. Distinct membrane domains on endosomes in the recycling pathway visualized by multicolor imaging of Rab4, Rab5, and Rab11. *J Cell Biol* **149:** 901–914.

Sotelo JR, Porter KR. 1959. An electron microscope study of the rat ovum. *J Biophys Biochem Cytol* **5:** 327–342.

Steinberg F, Gallon M, Winfield M, Thomas EC, Bell AJ, Heesom KJ, Tavare JM, Cullen PJ. 2013. A global analysis of SNX27–retromer assembly and cargo specificity reveals a function in glucose and metal ion transport. *Nat Cell Biol* **15:** 461–471.

Stenmark H. 2009. Rab GTPases as coordinators of vesicle traffic. *Nat Rev Mol Cell* **10:** 513–525.

Stoorvogel W, Strous GJ, Geuze HJ, Oorschot V, Schwartz AL. 1991. Late endosomes derive from early endosomes by maturation. *Cell* **65:** 417–427.

Stoorvogel W, Oorschot V, Geuze HJ. 1996. A novel class of clathrin-coated vesicles budding from endosomes. *J Cell Biol* **132:** 21–33.

Studer D, Graber W, Al-Amoudi A, Eggli P. 2001. A new approach for cryofixation by high pressure freezing. *J Microsc* **203:** 285–294.

Stuffers S, Sem Wegner C, Stenmark H, Brech A. 2009. Multivesicular endosome biogenesis in the absence of ESCRTs. *Traffic* **10:** 925–937.

Swanson J, Bushnell A, Silverstein SC. 1987. Tubular lysosome morphology and distribution within macrophages depend on the integrity of cytoplasmic microtubules. *Proc Natl Acad Sci* **84:** 1921–1925.

Taguchi T. 2013. Emerging roles of recycling endosomes. *J Biochem* **153:** 505–510.

* ten Broeke T, Wubbolts R, Stoorvogel W. 2013. MHC class II antigen presentation by dendritic cells regulated through endosomal sorting. *Cold Spring Harb Perspect Biol* **5:** a016873.

Theos AC, Tenza D, Martina JA, Hurbain I, Peden AA, Sviderskaya EV, Stewart A, Robinson MS, Bennett DC, Cutler DF, et al. 2005. Functions of AP-3 and AP-1 in tyrosinase sorting from endosomes to melanosomes. *Mol Biol Cell* **16:** 5356–5372.

Theos AC, Truschel ST, Tenza D, Hurbain I, Harper DC, Berson JF, Thomas PC, Raposo G, Marks MS. 2006. A lumenal domain-dependent pathway for sorting to intralumenal vesicles of multivesicular endosomes involved in organelle morphogenesis. *Dev Cell* **10:** 343–354.

Tooze J, Hollinshead M. 1991. Tubular early endosomal networks in AtT20 and other cells. *J Cell Biol* **115:** 635–653.

* Tooze SA, Abada A, Elazar Z. 2014. Endocytosis and autophagy. Exploitation or cooperation? *Cold Spring Harb Perspect Biol* doi: 10.1101/cshperspect.a018358.

Trajkovic K, Hsu C, Chiantia S, Rajendran L, Wenzel D, Wieland F, Schwille P, Brugger B, Simons M. 2008. Ceramide triggers budding of exosome vesicles into multivesicular endosomes. *Science* **319:** 1244–1247.

Traub LM, Bannykh SI, Rodel JE, Aridor M, Balch WE, Kornfeld S. 1996. AP-2-containing clathrin coats assemble on mature lysosomes. *J Cell Biol* **135:** 1801–1814.

Trowbridge IS. 1991. Endocytosis and signals for internalization. *Curr Opin Cell Biol* **3:** 634–641.

Ullrich O, Reinsch S, Urbe S, Zerial M, Parton RG. 1996. Rab11 regulates recycling through the pericentriolar recycling endosome. *J Cell Biol* **135:** 913–924.

Urbe S, Sachse M, Row PE, Preisinger C, Barr FA, Strous G, Klumperman J, Clague MJ. 2003. The UIM domain of Hrs couples receptor sorting to vesicle formation. *J Cell Sci* **116:** 4169–4179.

van Dam EM, Stoorvogel W. 2002. Dynamin dependent transferrin receptor recycling by endosome-derived clathrin-coated vesicles. *Mol Biol Cell* **13:** 169–182.

Van der Sluijs P, Hull P, Webster P, Male P, Goud B, Zerial M. 1992. The small GTP-binding protein Rab4 controls an early sorting event on the endocytic pathway. *Cell* **70:** 729–740.

van Niel G, Wubbolts R, ten Broeke T, Buschow SI, Ossendorp FA, Melief CJ, Raposo G, van Balkom BW, Stoorvogel W. 2006. Dendritic cells regulate exposure of MHC class II at their plasma membrane by oligoubiquitination. *Immunity* **25:** 885–894.

van Niel G, Charrin S, Simoes S, Romao M, Rochin L, Saftig P, Marks MS, Rubinstein E, Raposo G. 2011. The Tetraspanin CD63 regulates ESCRT-independent and -dependent endosomal sorting during melanogenesis. *Dev Cell* **21:** 708–721.

van Rijnsoever C, Oorschot V, Klumperman J. 2008. Correlative light-electron microscopy (CLEM) combining

live-cell imaging and immunolabeling of ultrathin cryosections. *Nat Methods* **5:** 973–980.

van Weering JR, Brown E, Sharp TH, Mantell J, Cullen PJ, Verkade P. 2010. Intracellular membrane traffic at high resolution. *Meth Cell Biol* **96:** 619–648.

van Weering JR, Sessions RB, Traer CJ, Kloer DP, Bhatia VK, Stamou D, Carlsson SR, Hurley JH, Cullen PJ. 2012. Molecular basis for SNX-BAR-mediated assembly of distinct endosomal sorting tubules. *EMBO J* **31:** 4466–4480.

* Wandinger-Ness A, Zerial M. 2014. Rab proteins and the compartmentalization of the endosomal system. *Cold Spring Harb Perspect Biol* doi: 10.1101/cshperspect.a022616.

Westlake CJ, Baye LM, Nachury MV, Wright KJ, Ervin KE, Phu L, Chalouni C, Beck JS, Kirkpatrick DS, Slusarski DC, et al. 2011. Primary cilia membrane assembly is initiated by Rab11 and transport protein particle II (TRAPPII) complex-dependent trafficking of Rabin8 to the centrosome. *Proc Natl Acad Sci* **108:** 2759–2764.

White IJ, Bailey LM, Aghakhani MR, Moss SE, Futter CE. 2006. EGF stimulates annexin 1–dependent inward vesiculation in a multivesicular endosome subpopulation. *EMBO J* **25:** 1–12.

Wilcke M, Johannes L, Galli T, Mayau V, Goud B, Salamero J. 2000. Rab11 regulates the compartmentalization of early endosomes required for efficient transport from early endosomes to the *trans*-Golgi network. *J Cell Biol* **151:** 1207–1220.

Willingham MC, Pastan I. 1980. The receptosome: An intermediate organelle of receptor mediated endocytosis in cultured fibroblasts. *Cell* **21:** 67–77.

Willingham MC, Pastan I. 1983. Formation of receptosomes from plasma membrane coated pits during endocytosis: Analysis by serial sections with improved membrane labeling and preservation techniques. *Proc Natl Acad Sci* **80:** 5617–5621.

Willingham MC, Hanover JA, Dickson RB, Pastan I. 1984. Morphologic characterization of the pathway of transferrin endocytosis and recycling in human KB cells. *Proc Natl Acad Sci* **81:** 175–179.

Yamashiro DJ, Tycko B, Fluss SR, Maxfield FR. 1984. Segregation of transferrin to a mildly acidic (pH 6.5) para-Golgi compartment in the recycling pathway. *Cell* **37:** 789–800.

Yu L, McPhee CK, Zheng L, Mardones GA, Rong Y, Peng J, Mi N, Zhao Y, Liu Z, Wan F, et al. 2010. Termination of autophagy and reformation of lysosomes regulated by mTOR. *Nature* **465:** 942–946.

Yudowski GA, Puthenveedu MA, Henry AG, von Zastrow M. 2009. Cargo-mediated regulation of a rapid Rab4-dependent recycling pathway. *Mol Biol Cell* **20:** 2774–2784.

Zeigerer A, Gilleron J, Bogorad RL, Marsico G, Nonaka H, Seifert S, Epstein-Barash H, Kuchimanchi S, Peng CG, Ruda VM, et al. 2012. Rab5 is necessary for the biogenesis of the endolysosomal system in vivo. *Nature* **485:** 465–470.

Zerial M, McBride H. 2001. Rab proteins as membrane organizers. *Nat Rev Mol Cell Biol* **2:** 107–119.

Zeuschner D, Geerts WJ, van Donselaar E, Humbel BM, Slot JW, Koster AJ, Klumperman J. 2006. Immuno-electron tomography of ER exit sites reveals the existence of free COPII-coated transport carriers. *Nat Cell Biol* **8:** 377–383.